Mean-Field Theory of Block Copolymers: Bulk Melts, Surfaces, and Thin Films

Kenneth R. Shull

IBM Almaden Research Center, 650 Harry Road, San Jose, California 95120

Received September 18, 1991; Revised Manuscript Received December 17, 1991

ABSTRACT: A quantitative mean-field treatment of inhomogeneous polymer systems is applied to bulk diblock copolymer melts, as well as to surfaces and thin films of these melts. Equations for a set of polymer chain probability distribution functions are solved numerically in a manner that requires no further approximation to the fundamental mean-field treatment. Results for symmetric block copolymer melts are in quantitative agreement with previous predictions which are valid only near the critical point or in the strong segregation regime. The equilibrium repeat period of bulk melts is found to scale as $R_g(\chi N)^{\alpha}$, where α varies continuously from 0.45 at the critical point to 0.17 in the strong segregation regime. Surfaces of block copolymer melts are treated in a quantitative fashion for films that are ordered or disordered in the bulk. Interference between composition oscillations originating from separate surfaces of a thin film induces thickness oscillations in the total interfacial free energy of the film. For symmetric block copolymer films, the free energy minima and maxima sharpen continuously as χN is increased through the value corresponding to the bulk critical point. A novel thickness instability mechanism is proposed by which a very thin film with an initial thickness corresponding to a broad free energy maximum will gradually evolve into a film containing regions of different thicknesses.

I. Introduction

Block copolymers have been the subject of extensive experimental and theoretical study, primarily because of the unique type of phase separation which can occur in these systems. The length scale of phase separation is controlled by the connectivity of repeat units along a polymer chain, with copolymers consisting of immiscible blocks forming ordered microdomain morphologies. Many practical applications of block copolymers make use of this intrinsic length scale, even if an ordered three-dimensional morphology is not formed. Examples include the stabilization of a dispersion by adsorption of a diblock copolymer onto the particle surfaces, where attractive van der Waals interactions are overwhelmed by repulsive osmotic interactions.[1] Use of diblock copolymers to enhance adhesion between immiscible homopolymers is a second example.[2] In this case the number of molecular entanglements between phases is enhanced by the extension of different copolymer blocks into opposing homopolymer matrix phases.[3]

While these and many other applications of block copolymers make use of unique surface or interfacial properties, a basic understanding of block copolymer thermodynamics must nevertheless begin with an understanding of bulk melts. Theories of bulk block copolymer melts have traditionally been divided into two classes: weak segregation theories, which are valid near the order–disorder transition where the magnitude of the composition oscillation is small, and strong segregation theories, which are valid in the well-ordered state where the interface between microdomains is small in comparison to the microdomain size. Nearly all of these theories are mean-field theories which neglect the importance of fluctuations in the local composition from an average value.

The distinction between strong and weak segregation mean-field theories arises primarily from approximations which are made to obtain mathematically tractable results. Consider, for example, the weak segregation theory of Leibler[4] and the strong segregation theory of Helfand and co-workers.[5,6] The Leibler theory describes the transition to an ordered phase from a disordered phase where the chain statistics are Gaussian and is based on the expansion of the free energy in powers of an order parameter. This order parameter is equal to the deviation in the local composition from the spatially averaged composition, and the treatment is quantitative when this order parameter is small, as is the case near the order–disorder transition. Scattering functions in the disordered phase are predicted by the theory, and the spinodal is obtained as the locus of points for which the scattering function diverges. For symmetric diblock copolymers the spinodal corresponds to a second-order transition from the disordered phase to the ordered phase.

The strong segregation theory of Helfand and co-workers is based on the use of direct space distribution functions which describe the probabilities of finding chain-end segments of different lengths at different positions. Deviations from the ideal Gaussian chain conformations are taken into account quantitatively by the introduction of a spatially varying mean field. Helfand and Wasserman introduce approximations which enable them to obtain analytic expressions for the free energy of an ordered lamellar phase.[6] These approximations are valid only in the strong segregation regime, although the basic underlying framework is valid for any ordered or disordered phase. For a homogeneous disordered phase the mean field is uniform and the ideal Gaussian chain statistics are recovered. The information obtained for the disordered phase is trivial, however, since no information is obtained with regard to the scattering functions.

Fredrickson extended the Leibler theory to take into account the effect of a single surface which has a preferential affinity for A (or B) repeat units.[7] This type of interaction was found to induce composition oscillations near the surface even when the bulk copolymer is disordered. These oscillations are characterized by a decay length which is predicted to diverge at the critical point. Thin films, where two surfaces are separated by a distance similar to the decay length of the composition oscillations, were not discussed by Fredrickson, although they are of experimental interest. Recent experiments by Russell et al. have shown that the thickness of copolymer films in the ordered state is quantized; i.e., the free energy of the copolymer film is minimized for thicknesses where composition oscillations emanating from both surfaces are in

0024-9297/92/2225-2122$03.00/0

phase with one another.[8] These results pertain to films which order in the bulk state such that the composition oscillations are characterized by an infinite decay length. Qualitatively similar results are expected whenever the overall film thickness is less than this decay length.

The work described in the present paper is a unifying mean-field theory of lamellar block copolymer melts which is applicable to bulk melts, melt surfaces, and thin films and is equally valid in the strong segregation and weak segregation regimes. As described in section II, the free energies and composition profiles are determined quantitatively, since no approximations are made in addition to the basic mean-field approximation. In section III results for symmetric diblock copolymer melts are presented for both weak and strong ordering. These results reduce to those of Helfand and Wasserman in the strong segregation regime and to those of Leibler at the order–disorder transition. Surface effects are discussed in section IV, followed by a discussion of thin films in section V. For thick films and small values of the order parameter, the results reduce to the analytic results of Fredrickson. For thin films the overall interfacial free energy is an oscillatory function of the film thickness, both above and below the disorder transition.

II. Theoretical Development

The theory is an extension of the theory of Helfand and co-workers[5,6,9-11] and is similar to the theories of Scheutjens and Fleer[12,13] and Hong and Noolandi.[14] The notation used in the present work is consistent with a previous theory of end-adsorbed polymers in polymeric matrices.[15] Details of the theoretical formulation are presented in this reference. The lamellar systems considered presently have planar symmetry, with the only relevant direction being that in which the composition varies. The system is broken up into layers along this direction, with the width of each layer being equal to **a**, the statistical length of a polymer chain repeat unit. This statistical length is defined such that R_g, the unperturbed radius of gyration of a copolymer chain, is equal to $(N/6\mathbf{a})^{1/2}$, where N is the number of repeat units in the copolymer chain. The layers in the system are represented by the index i, and the different repeat units of a given polymer chain are represented by the index j. Polymer chain probability distribution functions, $q(i,j)$, are the central quantities of the theory. These distribution functions are related to the probability of finding the termination of a chain segment of length j within layer i. Chain segments are defined such that they begin from a given end of a copolymer chain, with separate distribution functions corresponding to the two distinct copolymer chain ends. Segments originating from the A end of the diblock copolymer are characterized by q_1, whereas segments originating from the B end are characterized by q_2. Connectivity of repeat units along the copolymer chain dictates that a chain segment of length j exists in a given layer only when a segment of length $j-1$ exists in the same layer or in one of the two adjacent layers. The following recursion relations are obtained for q_1 and q_2

$$q_1(i,j) = \left\{\frac{1}{6}q_1(i-1,j-1) + \frac{1}{6}q_1(i+1,j-1) + \frac{4}{6}q_1(i,j-1)\right\}\exp\{-w(i,j)/k_BT\} \quad (1)$$

$$q_2(i,j) = \left\{\frac{1}{6}q_2(i-1,j-1) + \frac{1}{6}q_2(i+1,j-1) + \frac{4}{6}q_2(i,j-1)\right\}\exp\{-w(i,j)/k_BT\} \quad (2)$$

where the distribution functions are set equal to 1 at $j = 0$:

$$q_1(i,0) = q_2(i,0) = 1 \quad (3)$$

As described previously[15] the distribution functions are discrete representations of the following modified diffusion equation developed by Edwards[16] and utilized in the theories of Helfand and co-workers,[5,6,9-11] Hong and Noolandi,[14] and others:

$$\frac{dq(x,n)}{dn} = \frac{\mathbf{a}^2}{6}\frac{d^2q(x,n)}{dn^2} - w(x,n)q(x,n) \quad (4)$$

Here the discrete variables i and j have been replaced by the continuous variables x and n, respectively. The correspondence between eq 4 and eqs 1 and 2 becomes exact as **a** becomes vanishingly small; i.e, eq 4 represents the continuous chain limit of eqs 1 and 2.[15] Equation 4 must in general be solved by numerical techniques which involve discretization of x and n. Equations 1 and 2 represent a specific discretization scheme which helps clarify the origin of the mathematics. Solutions presented in the following sections are indistinguishable from results obtained in the continuous chain limit.

The j dependence of the local mean fields is entirely determined by the species (A or B) represented by the jth repeat unit. We consider a diblock copolymer which contains gN repeat units of type A followed by $(1-g)N$ repeat units of type B. Equation 1 for q_1 therefore has $w(i,j) = w_a(i)$ for j ranging from 1 to gN and $w(i,j) = w_b(i)$ for j ranging from $gN+1$ to N. Similarly, eq 2 for q_2 has $w(i,j) = w_b(i)$ for j ranging from 1 to $(1-g)N$ and $w(i,j) = w_a(i)$ for j ranging from $(1-g)N+1$ to N. These mean fields, w_a for A repeat units and w_b for B repeat units, are given by the expressions

$$w_a(i) = k_BT\chi\phi_b^2(i) - \Delta w(i) \quad (5)$$

$$w_b(i) = k_BT\chi\phi_a^2(i) - \Delta w(i) - w_{ext}(i) \quad (6)$$

where ϕ_a and ϕ_b are the local volume fractions of A and B repeat units, χ is the Flory interaction parameter characterizing the thermodynamic interaction between A and B repeat units, and w_{ext} is an external field imposed, for example, by a free surface. The incompressibility constraint is accounted for in the quantity Δw, which is given by

$$\Delta w(i) = \zeta\{1 - \phi_a(i) - \phi_b(i)\} \quad (7)$$

Here ζ is a parameter that is inversely proportional to the compressibility of the copolymer melt. Values of ζ for real polymers are high enough so that the results obtained from the mean-field calculations are indistinguishable from the limiting incompressible case corresponding to $\zeta = \infty$.[9,10]

The local volume fractions of A and B repeat units are given by

$$\phi_a(i) = \frac{1}{N}\exp(\mu'/k_BT)\sum_{j=1}^{gN} q_1(i,j)q_2(i,N-j) \quad (8)$$

$$\phi_b(i) = \frac{1}{N}\exp(\mu'/k_BT)\sum_{j=1}^{(1-g)N} q_2(i,j)q_1(i,N-j) \quad (9)$$

The quantity μ' can be viewed as an effective chemical potential of a copolymer chain. The remainder of the free

energy is accounted for in γ, a term that is analogous to an interfacial free energy

$$\gamma = a\rho_0 \sum_{i=1}^{L'} \Delta w(i) \tag{10}$$

where there are a total of L' layers in the system. The free energy density of the system, f, is given by adding the contribution from the chemical potential to γ and then dividing by $L'\mathbf{a}$, the width of the system:

$$f = \frac{\rho_0}{L'} \sum_{i=1}^{L'} \{\Delta w(i) + \mu'/N\} \tag{11}$$

The actual free energy per copolymer chain, μ, is given by multiplying f by N/ρ_0, the volume of a copolymer chain:

$$\mu = \mu' + \frac{N}{L'} \sum_{i=1}^{L'} \Delta w(i) \tag{12}$$

Pure polymers in the absence of the thermodynamic interaction characterized by χ serve as the reference state for this free energy density. The free energy density f_0 of a homogeneous copolymer melt with respect to this same reference state is given by the familiar regular solution form:

$$\frac{f_0}{k_B T} = \rho_0 \chi \phi_a \phi_b = \rho_0 \chi g(1-g) \tag{13}$$

Extension of the theory to multicomponent systems is straightforward, as is extension to the case where the characteristic chain dimensions for different repeat unit types are no longer identical. These generalizations are described in the appendixes. In the following sections we illustrate some of the fundamental features of pure diblock copolymer melts by applying the theory to the completely symmetric case, where the volumes and radii of gyration of the two blocks are identical.

III. Properties of Bulk Melts

Periodic lamellar microdomain morphologies are studied by utilizing the following boundary condition for the distribution functions:

$$q(i, j) = q(i + L', j) \tag{14}$$

Equations 1–3, 5–9, and 14 form a closed set of equations which are solved numerically by a relaxation method as described previously.[3] It is most convenient to use a normalized repeat period L/R_g, where L is the actual copolymer repeat period. The distance corresponding to L' lattice layers is $L'\mathbf{a}$, and the radius of gyration of a copolymer chain is given by $\mathbf{a}(N/6)^{1/2}$. The quantity L/R_g is therefore obtained from L' by dividing by $(N/6)^{1/2}$. Calculated values of the free energy per copolymer chain are plotted in Figure 1 as a function of L/R_g for values of χN ranging from 12 to 80. The minima in these free energy curves represent the equilibrium repeat periods for the corresponding values of χN.

The normalized equilibrium repeat periods are plotted in Figure 2 as a function of χN. Helfand and Wasserman have given an analytic expression for the free energy per chain which is accurate for high values of χN.[6] The approximation made in the derivation of this analytic free energy expression is that the interphase region between

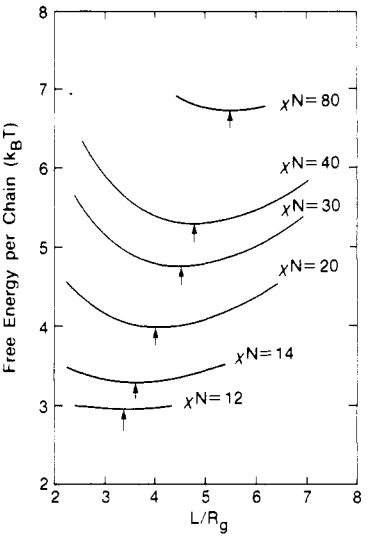

Figure 1. Calculated values of the free energy per chain as a function of the repeat period of a symmetric lamellar microdomain morphology. Equilibrium values for the repeat period correspond to the free energy minima indicated by the arrows.

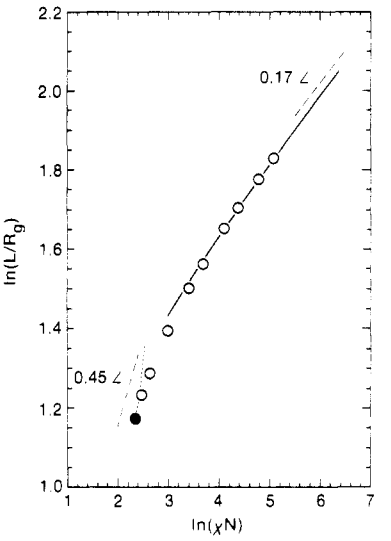

Figure 2. Equilibrium repeat period for a symmetric lamellar microdomain morphology as a function of χN. Open circles represent values obtained from minima of free energy curves such as those shown in Figure 1. The solid symbol represents the Leibler prediction for the critical point (L/R_g = 3.23 at χN = 10.5),[4] and the solid line represents the Helfand and Wasserman prediction from the narrow interphase approximation.[6] The dotted line represents the weak segregation prediction of Mayes and Olvera de la Cruz.[20,21]

pure A and B microdomains is much narrower than the width of a microdomain. Minimization of the free energy expression derived from this "narrow interphase approximation" gives the solid line shown in Figure 2. The narrow interphase approximation gives quantitatively correct values for L provided that χN is greater than 40, as demonstrated by Helfand and Wasserman in their original paper.[6] In the strong segregation regime where the narrow interphase approximation is valid, the scaling relationship

$$L/R_g = C(\chi N)^{1/6} \tag{15}$$

is obtained, where C is a constant. Since R_g is proportional to $N^{1/2}$, one has

$$L \propto \chi^{1/6} N^{2/3} \tag{16}$$

which is the well-known scaling result characterizing the

strong segregation regime for lamellar diblock copolymers. This result can be obtained in a simple manner by balancing the free energy associated with the interface between the microdomains against the energy associated with the stretching of the chains away from the interface. A detailed derivation of eq 15 has been given by Semenov.[17] His value of 2.69 for the constant factor C gives a result for L/R_g as a function of χN that is virtually identical to the Helfand and Wasserman prediction plotted in Figure 2.

Equilibrium volume fractions of B repeat units across a repeat period are shown in Figure 3 for three values of χN. For values of χN that are no greater than 12, the concentration profile is nearly a perfect sine wave superimposed on the average composition ($\phi_a = \phi_b = 0.5$). The magnitude of this sine wave decreases steadily as χN is decreased further and vanishes continuously at the critical point. Plots of the free energy per chain as a function of L/R_g also become flatter as the mean-field critical point is approached. At this critical point the copolymer melt is homogeneous, and there is no curvature at all from which to extract the equilibrium value of L/R_g. Leibler obtained values of L/R_g and χN at the critical point by examining the properties of the copolymer scattering function in the mean-field approximation.[4] In general, the value of χN at the spinodal is the value for which the scattering function diverges, with the equilibrium value of L/R_g being directly related to the magnitude of the scattering vector which shows divergent behavior. For the symmetric case considered here, the spinodal corresponds to the critical point at $\chi N = 10.495$, with $L/R_g = 3.23$.

For $\chi N > 20$ the lamellar copolymer microphases consist of pure A and B microdomains separated by an interfacial region of width w. The composition across this interfacial region is closely approximated by a hyperbolic tangent profile

$$\phi_b(x) = -0.5 \tanh\left\{\frac{2(0.25L - x)}{w}\right\} + 0.5 \tanh\left\{\frac{2(0.75L - x)}{w}\right\} \quad (17)$$

where w is a measure of the interfacial width and is equal to the inverse of the maximum slope of the concentration profile:

$$w = \left\{\frac{d\phi_b(x)}{dx}\right\}^{-1}_{x/L=0.25} \quad (18)$$

In the limit of infinite χN, the interface between the immiscible A and B copolymer blocks is identical to the interface between homopolymers of infinite molecular weight. In this asymptotic limit the self-consistent solution to the mean-field equations can be determined analytically, in which case one obtains the following for w_∞, the asymptotic value of the interfacial width:[9]

$$w_\infty = 2a/(6\chi)^{1/2} = 2R_g/(\chi N)^{1/2} \quad (19)$$

For finite values of χN, the interfacial width is greater than w_∞ due to the added constraint that the joint between the copolymer blocks be located within the interfacial region. This constraint introduces an additional positive term in the free energy which increases with decreasing w. As χN and L/R_g approach infinity, the number of copolymer joints becomes vanishingly small, such that w_∞ is reached as the asymptotic limit. Figure 4 shows how this asymptotic limit is approached as χN is increased.

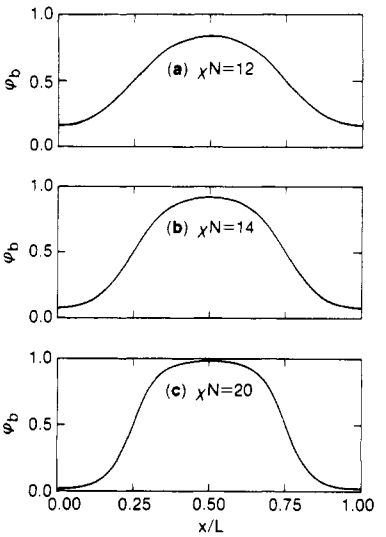

Figure 3. Calculated composition profiles for a symmetric lamellar morphology with $\chi N = 12$, 14, and 20.

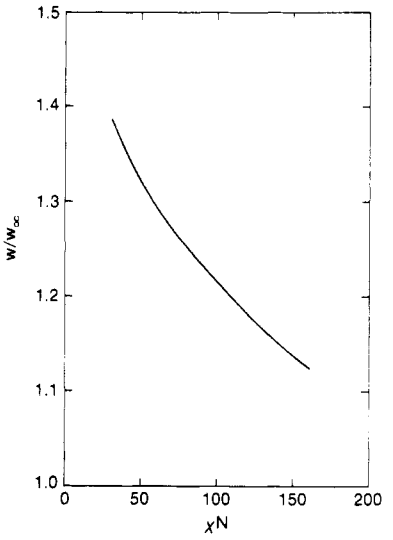

Figure 4. Width of the interphase region for a symmetric lamellar morphology as a function of χN. The width is normalized by w_∞, the width of the interface between infinite molecular weight homopolymers ($w_\infty = 2a/(6\chi)^{1/2}$).

The actual interfacial width is noticeably larger than w_∞, well into the strong segregation regime.

Figures 1–4 summarize the mean-field predictions for bulk, symmetric diblock copolymers. Much of what is included in these figures has already been determined from previous theoretical treatments. New results include the deviations of the interdomain width from its asymptotic value and the behavior of the symmetric block copolymers in the crossover regime between the critical point and the strong segregation regime. Illustration of the mean-field behavior in this crossover regime is perhaps the most important aspect of the current treatment. This crossover regime, typically referred to as the weak segregation regime, is characterized by a dependence of L/R_g on χN which is stronger than that observed for the strong segregation regime. If one characterizes the relationship between these two quantities by the exponent α, such that $L/R_g \propto (\chi N)^\alpha$, then Figure 2 shows that α decreases continuously from a value of 0.45 at the critical point to a value of $\cong 0.17$ in the strong segregation regime. Equivalently, the exponent characterizing the relationship between L and N for a given polymer decreases from 0.95 to 0.67 as one moves into the strong segregation regime.

In mean-field theory the only relevant length scale for the disordered phase is the copolymer radius of gyration. The length scales of all correlations in the disordered phase are therefore predicted to be independent of χ and to scale as $N^{0.5}$. It has often been assumed that a similar scaling holds in the weak segregation regime, in which case L/R_g would be independent of χN. Figure 2 clearly shows that this is not the case and that L varies linearly with R_g only when χN is held constant. The true mean-field prediction is that the N dependence of the repeat period is stronger in the weak segregation regime than in the strong segregation regime. The weak $N^{1/2}$ dependence is not characteristic of weak segregation but is instead characteristic of the completely homogeneous phase where there is no ordering whatsoever. This picture is complicated by the appearance of composition fluctuations in the disordered phase, as mentioned under Discussion.

IV. Surface Properties

A surface is introduced into the mean-field equations by replacing the periodic boundary condition at $i = 0$ with the requirement that the distribution functions vanish at $i = 0$. For $\chi N < 10.5$ the bulk phase is homogeneous, and the boundary condition at $i = L$ is replaced with the condition that $\Delta w(L) = 0$. A preferential affinity of the surface for the B component is included by setting $w_{ext}(i)$ to some positive value for $i = 1$, with $w_{ext}(i) = 0$ for $i > 1$. In theories of polymer blend surfaces, a bare surface free energy F_s is typically introduced into the problem.[7,18] The driving force for segregation of B repeat units to the surface is the derivative of F_s with respect to the surface volume fraction of the B species, which can be expressed in terms of the phenomenological parameters μ_1 and g^* as follows:

$$-\frac{\partial F_s}{\partial \phi_1} = \rho_0 k_B T\{\mu_1 + g^*\phi_1\} \tag{20}$$

Here ϕ_1 represents the surface volume fraction of B repeat units and ρ_0 is the concentration of repeat units, i.e., the inverse of the repeat unit volume. Equation 20 defines the quantities μ_1 and g^*. These quantities have dimensions of length, with their magnitudes depending on how a repeat unit is defined. The quantity $w_{ext}(1)$ represents the free energy gain associated with the exchange of a B repeat unit for an A repeat unit in the first layer. In the lattice treatment used here the surface field extends over a single lattice layer. The width of this layer is **a**, the statistical length of a repeat unit, such that the areal density of segments which feel the surface field is $\mathbf{a}\rho_0$. The quantity $\partial F_s/\partial \phi_1$ is therefore related to $w_{ext}(1)$ in the following manner:

$$-\frac{\partial F_s}{\partial \phi_1} = \mathbf{a}\rho_0 w_{ext}(1) \tag{21}$$

Comparison of eqs 20 and 21 gives $w_{ext}(1)/k_BT = (\mu_1 + g^*\phi_1)/\mathbf{a}$. This relationship allows one to establish a connection to previous theories in which the surface interaction is expressed in terms of μ_1 and g^*.[7,18] The quantity g^* can be included in the present theory by allowing $w_{ext}(1)$ to be a function of $\phi_b(1)$. Nothing is gained from this extension, however, since the complete profile is specified only by $w_{ext}(1)$ or, alternatively, by $\partial F_s/\partial \phi_1$. The results described here are expressed in terms of $\partial F_s/\partial \phi_1$, since this is the straightforward driving force for surface ordering.

The effects of a surface on the properties of a symmetric diblock copolymer have been examined by Fredrickson,[7] using a treatment similar to that used by Leibler to describe the properties of bulk block copolymer in the weak segregation regime.[4] As with Leibler's treatment the predictions are quantitative only when deviations in the local composition from the average value ($\phi_b = 0.5$) are small. Fredrickson found that the effect of the surface is to induce sinusoidal composition oscillations which decay into the bulk as follows:

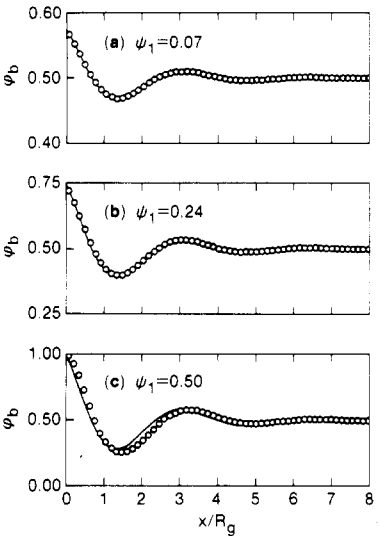

Figure 5. Surface profiles for a symmetric copolymer with $\chi N = 9$, for three different values of the surface order parameter $\psi_1(\psi_1 = \phi_1 - 0.5)$. Symbols represent the detailed mean-field prediction, whereas the solid lines represent the predictions of the Fredrickson weak segregation theory (eqs 22, 24–26).

$$\phi_b(x) = 0.5 + \frac{\psi_1}{\cos\phi}\exp(-x/\zeta)\cos(\Omega x + \phi) \tag{22}$$

Here ψ_1 is an order parameter describing the magnitude of the composition oscillation at the surface and is the only parameter that depends on $\partial F_s/\partial \phi_1$:

$$\psi_1 = (\partial F_s/\partial \phi_1)V/5.264R_g k_B T(1.515 - 0.144\chi N)^{1/2} \tag{23}$$

The phase shift ϕ is predicted to depend only on the proximity to the critical point

$$\tan\phi = \{(1.515 - 0.144\chi N)/(0.485 + 0.144\chi N)\}^{1/2} \tag{24}$$

whereas the oscillatory period Ω and the decay length ζ are predicted to depend on the proximity to the critical point and on the copolymer radius of gyration:

$$\zeta = R_g/1.316(1.515 - 0.144\chi N)^{1/2} \tag{25}$$

$$\Omega = (1.316/R_g)(0.485 + 0.144\chi N)^{1/2} \tag{26}$$

At the critical point ($\chi N = 10.5$) eq 25 predicts a divergence in the decay length, while eq 23 predicts a divergence in the magnitude of the composition oscillations for any finite value of $\partial F_s/\partial \phi_1$. The assumption that the composition oscillations are small is obviously breaking down in this regime. It is therefore beneficial to use the full mean-field treatment described in section II to determine the extent to which the analytic results of the Fredrickson theory are valid. Figure 5 shows a series of surface composition profiles for $\chi N = 9$ as determined by numerical solution of the mean-field equations of section II (symbols) and by the Fredrickson theory (solid lines). The three different curves correspond to three values of

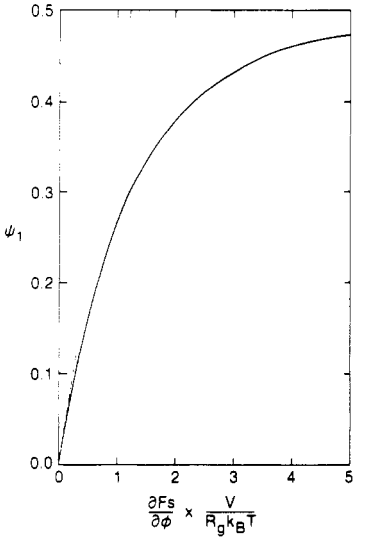

Figure 6. Surface order parameter as a function of $\partial F_s/\partial \phi_1$ for a symmetric copolymer with $\chi N = 9$. The solid line represents the prediction of the detailed mean-field theory which is valid for all values of ψ_1. The dashed line represents the prediction of the Fredrickson theory (eq 23), which is valid only when ψ_1 is small.

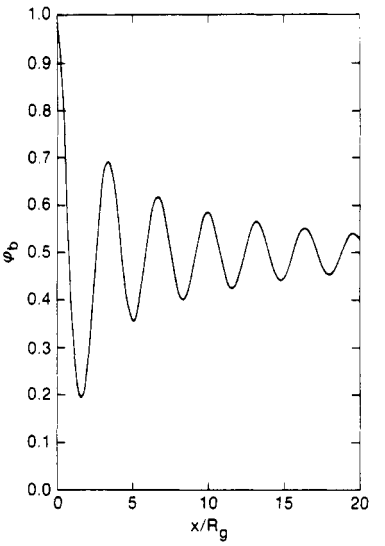

Figure 7. Calculated surface profile for a symmetric copolymer with $\phi_1 = 1$ and $\chi N = 10.5$.

the surface order parameter ψ_1. This parameter was varied independently to obtain the best fit to the Fredrickson theory, using the values of ϕ, ζ, and Ω given by eqs 24–26. As one would expect, agreement between the two treatments is quantitative when ψ_1 is small. A more surprising result is the extent to which the two treatments agree for values of the surface order parameter which approach the maximum value of 0.5. Figure 5 shows that the Fredrickson theory gives results which are nearly indistinguishable from the more accurate numerical results for $\psi_1 = 0.24$ and gives a reasonable result even for ψ_1 equal to the maximum value of 0.5.

This analysis shows that eqs 22 and 24–26 do a remarkable job of describing the mean-field surface properties of symmetric diblock copolymer melts, provided that χN is considerably less than the critical value of 10.5 and that the surface order parameter is given. The value of ψ_1 itself is overestimated by the Fredrickson theory, however, for any appreciable degree of surface order. This result is illustrated by Figure 6, where ψ_1 is plotted as a function of $\partial F_s/\partial \phi_1$ for a symmetric copolymer with $\chi N = 9$. The numerical mean-field results are represented by the solid line in Figure 6, whereas the Fredrickson prediction of eq 23 is represented by the dashed line. Deviations from the Fredrickson theory become significant for $\psi_1 \geq 0.1$.

As mentioned above, the decay length of small composition oscillations diverges at the critical point. This result is retained by the complete numerical solution of the mean-field equations, as indicated by the quantitative agreement with the Fredrickson theory for small values of the order parameter. The decay length of large composition oscillations induced by the presence of a free surface does not diverge at the critical point, however. Consider, for example, the surface of a symmetric diblock copolymer at its critical point ($\chi N = 10.5$), with $\partial F_s/\partial \phi_1$ large enough so that $\psi_1 = 0.5$. Figure 7 shows the calculated surface profile for such a block copolymer. The surface-induced order propagates well into the bulk of the polymer but is nevertheless characterized by a finite decay length. Oscillations decay more slowly as their magnitude decreases, a result which is consistent with the prediction that small oscillations are characterized by an infinite decay length for this polymer. The decay of the larger oscillations induced by the surface is a highly nonlinear effect which is taken into account automatically by numerical solution of the self-consistent mean-field equations.

V. Thin Films

Treatment of thin block copolymer films is a straightforward extension of the treatment of block copolymer surfaces. One must merely introduce a second surface by changing the boundary condition at $i = L'$. To illustrate some of the basic features of thin block copolymer films, we consider the situation where both surfaces are saturated with the B component of a symmetric block copolymer. Composition oscillations induced from each surface propagate toward the center of the film. The overall free energy of the film is determined by the manner in which these composition oscillations interfere with one another, with free energy minima corresponding to film thicknesses for which the oscillations reinforce one another. Equation 10 gives the overall interfacial free energy of such a thin film, provided that the quantity μ' is set equal to the actual free energy per chain in the corresponding bulk phase. For $\chi N < 10.5$ this free energy per chain is equal to $k_B T \chi N/4$ for a symmetric bulk copolymer. For $\chi N > 10.5$ the free energy per chain is obtained from the minimum in a free energy plot like those shown in Figure 1. Use of a different value for μ' introduces a contribution to γ which is linear in the film thickness and does not affect the analysis which follows.

Calculated values of the interfacial free energy as a function of the film thickness d are shown in Figure 8 for $\chi N = 9$, 10.5, and 12. For $\chi N = 9$ and 10.5 the plots represent deviations in the interfacial free energy from the interfacial free energy of a thick film. For $\chi N = 12$ the bulk film is ordered, and the plot represents the deviation in surface free energy from a series of discrete minima corresponding to film thicknesses equal to integral numbers of repeat periods. As χN is increased from 9 to 12, the characteristic maxima and minima in the free energy curves become sharper, with no discernible discontinuity at the bulk critical point.

Free energy minima for the most highly ordered film ($\chi N = 12$) occur at thicknesses of $3.82R_g$, $7.21R_g$, and $10.75R_g$. While the first free energy minimum is at a somewhat greater film thickness than the bulk equilib-

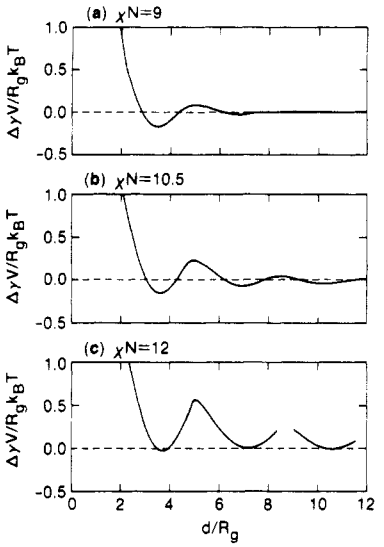

Figure 8. Normalized interfacial free energy for thin, symmetric diblock copolymer films with χN = 9, 10.5, and = 12. Each of the curves corresponds to the case where ϕ_1 = 1 for both film surfaces.

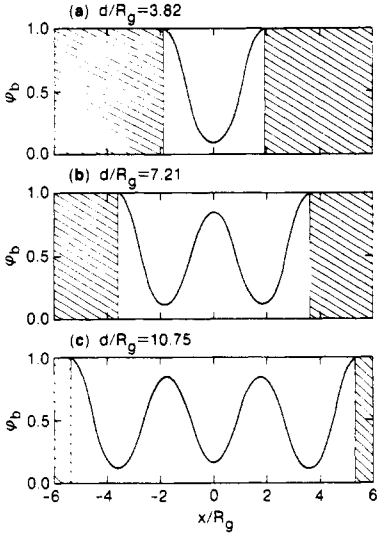

Figure 9. Calculated profiles for film thicknesses corresponding to the three free energy minima of Figure 8c (χN = 12).

rium repeat period of $3.42R_g$, the increment between the three different thickness minima is itself very close to this bulk repeat period. This is a sensible result and is consistent with the types of profiles that are obtained for these three thicknesses. These profiles are shown in Figure 9 and should be compared to the composition profile across a bulk repeat period shown in Figure 3a. The profile at d/R_g = 7.21 (Figure 9b) can be obtained from the profile at d/R_g = 3.82 (Figure 9a) by adding a single bulk repeat period. A similar relationship exists between the profiles shown in parts b and c of Figure 9. In each case the thickness increment is equal to a bulk repeat period. The first free energy minimum occurs at a thickness which is not equal to the bulk repeat period because of the different boundary condition: ϕ_b is equal to 1 at the surfaces of the thin film but has a maximum value of 0.84 in the bulk phase.

Free energy maxima for films that are ordered in a corresponding bulk phase occur at film thicknesses approximately equal to $(n + 1/2)L$, where n is an integer and L is the bulk repeat period. The exact position of the free energy maximum depends on the free energy penalty associated with compressing or expanding lamellae from

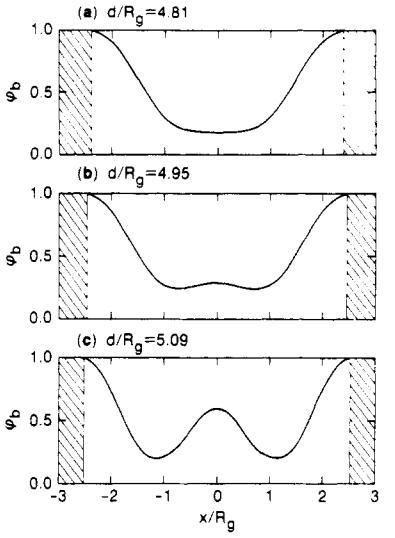

Figure 10. Calculated profiles for three film thicknesses near the first free energy maximum of Figure 8c (χN = 12).

their minimum free energy thicknesses. At the first free energy maxima (n = 1) small changes in film thickness have large effects on the structure of the thin film, as illustrated by the profiles shown in Figure 10. The three different profiles represent three film thicknesses in the vicinity of the first free energy maximum for a symmetric copolymer with χN = 12. For d/R_g = 4.81 (Figure 10a) the thin film contains a single period which is stretched from its equilibrium value. Similarly, for d/R_g = 5.09 (Figure 10c) the thin film contains two compressed periods. Intermediate values of d/R_g represent the continuous crossover from a film with a single period to a film with two periods as the film thickness increases. The continuous nature of the crossover is analogous to a second-order phase transition, with the film thickness acting, for example, as the temperature.

The transition from a single period to a double period is unique in that it represents a doubling of the periodicity which can be accomplished by the continuous evolution of a second peak in the composition profile as illustrated by Figure 10. Transitions occurring at subsequent free energy maxima (n > 1) are discontinuous. An expanded two-period film cannot, for example, be transformed into a compressed three-period film by any gradual transformation. Instead, the free energy of the two-period film increases with increasing film thickness until its free energy is higher than that of a three-period film of equivalent thickness. At this thickness the equilibrium profile across the film changes to the dramatically different three-period form, by analogy to a first-order phase transition.

First-order transitions present a unique theoretical challenge, since self-consistent solutions need to be obtained for each of the different states to compare the free energies. Self-consistent solutions do not necessarily represent the state of lowest possible free energy but instead represent states where the free energy is at a local minimum. Small perturbations to such a state will always increase the free energy, but large-scale rearrangements can potentially produce a state of decreased free energy. Second-order transitions are determined in a straightforward manner by a single set of self-consistent solutions since the properties of the system are varying continuously. In contrast, examination of a first-order transition requires that the self-consistent mean-field solution first be obtained for each different state. The location of the transition is then obtained by comparing the free energies of the different states. Obtaining convergence of the mean-

field equations to a desired state is not always straightforward, as it depends in a nontrivial way on the initial guess for the mean fields and on the iterative scheme used to obtain the final self-consistent solution. The gap in the free energy curve in Figure 8c is due to the tendency for the solution to converge on the two-period film for cases where the three-period film would actually have a lower energy.

VI. Discussion

In contrast to mean-field theories which apply only in the weak or strong segregation regimes, numerical solution of the mean-field equations of section II does not require that any additional approximations be made. The accuracy of the theory is therefore determined by the accuracy of the fundamental mean-field approximations upon which the equations are based. These approximations are to neglect the importance of fluctuations and to treat correlations between repeat units along a given polymer chain by considering only averaged quantities. In our case these quantities are the volume fractions, the mean fields, and the polymer chain distribution functions. Polymer chain connectivity is taken into account through relationships between the distribution functions, as illustrated by eqs 1 and 2. These relationships may in fact be altered by the connectivity of the surroundings, and these second-order effects are not included in the theory. This aspect of the mean-field approximation can be removed only by considering the average properties of an ensemble of completely connected polymer chains, i.e., by averaging after the polymer chain connectivity is taken into account. Inclusion of fluctuation effects requires that deviations from the average quantities be included in the expression for the free energy, as in the recent fluctuation theory of Fredrickson and Helfand.[19]

The theories of Leibler[4] and of Helfand and Wasserman[6] neglect fluctuations and treat correlations in the same manner as they are treated here. Differences between these three treatments reside only in the nature of additional approximations which are made in the Leibler and Helfand–Wasserman theories. The strong segregation theory of Helfand and Wasserman is based on the solution of mean-field equations which are identical to those given in section II. It is obvious, therefore, that the fundamental mean-field approximation made by Helfand and Wasserman is identical to the mean-field approximation employed here. The narrow interphase approximation is an additional approximation which Helfand and Wasserman introduce to obtain useful analytic results. This additional approximation is valid only for high values of χN, and it is for this reason that the results of Helfand and Wasserman cannot be accurately extended into the weak segregation regime.

Leibler's weak segregation theory is based on the expansion of the free energy about the free energy of a homogeneous phase. The free energy expansion is obtained in terms of the Fourier components of the order parameter

$$f = f_0 + k_B T \sum_{n=2}^{\infty} \frac{V^{-n}}{n!} \sum_{(q_1,\ldots,q_n)} \Gamma_n(q_1, \ldots, q_n)\psi(q_1)\ldots\psi(q_n) \qquad (27)$$

with $\psi(q) = \int_V \psi(x)e^{iqx}$ and $\psi(x) = \phi(x) - g$. The values of χN and L/R_g which correspond to the critical point are determined by the second-order term in the free energy expansion of eq 27. Inclusion of this term as given by Leibler gives

$$f = f_0 + \frac{k_B T}{2NV} \sum_q \{F(q^2 R_g^2) - 2\chi N\}\psi^2(q) \qquad (28)$$

where $F(x)$ is given by

$$F(x) = \frac{g_1(1, x)}{g_1(g, x)g_1(1-g, x) - \frac{1}{4}[g_1(1, x) - g_1(g, x) - g_1(1-g, x)]^2} \qquad (29)$$

with g_1 being the Debye function:

$$g_1(g, x) = 2\{gx + \exp(-gx) - 1\}/x^2 \qquad (30)$$

The function $F(x)$ has a minimum value of 20.99 at $x = 3.78$. The equilibrium repeat period at the order–disorder transition is therefore given by the condition $q^2R_g^2 = 3.78$. Since $L = 2\pi/q$, we have $L/R_g = 3.23$. The value of χN at the order–disorder transition is the value for which $f = f_0$, with $F(x)$ equal to its minimum value. Inspection of eq 28 shows that this value is $20.99/2 = 10.495$. At the critical point the order parameter is vanishingly small, and the approximation associated with the truncation of the expansion of eq 27 becomes exact. The only approximation made in the determination of the critical point is therefore the mean-field approximation from which the form of the second-order term in the free energy expansion is derived. This approximation is identical to the mean-field approximation upon which the equations of section II are based, so it is not surprising that both techniques give the same results at the critical point.

Extension of results obtained from a treatment similar to that of Leibler to higher values of χN, where the order parameter is finite, requires that higher order terms in the free energy expansion of eq 27 be included. The third- and fourth-order terms were calculated by Leibler, but the effect of their inclusion on the value of the equilibrium repeat period was not calculated in his original treatment. Mayes and Olvera de la Cruz have recently obtained the weak segregation prediction for L/R_g as a function of χN by including these terms in the free energy expansion.[20] Their prediction is shown as the dotted line in Figure 2.[21] For $\chi N = 12$ (the first open symbol on Figure 2), the maximum order parameter is significant, as indicated by the profile shown in Figure 3a. At this point terms higher than fourth order in the free energy expansion of eq 27 become important and the fourth-order expansion breaks down. Contributions of higher harmonics to the composition profile and to the free energy were also included by Mayes and Olvera de la Cruz but were found to be quite small, as one would expect from the nearly sinusoidal nature of the calculated profile shown in Figure 3a. For symmetric copolymers, therefore, the fourth-order expansion breaks down before the contributions of higher order harmonics become important.

Melenkevitz and Muthukumar have also used an extension of the Leibler theory to study the properties of symmetric diblock copolymer melts.[22] They extend their treatment into the strong segregation regime by including a very large number of terms in the Fourier expansion of the composition profile. The free energy expansion is truncated after the fourth-order terms, and the wave vector dependence of the coefficients in the expansion is neglected. The Fourier coefficients of the composition profile are also assumed to obey a relatively simple form in order that the free energy minimization can be accomplished.

Truncation of the free energy expansion, approximation of the coefficients in the expansion, and constraint of the form of the composition profile all represent approximations which affect the results. It is for this reason that the results of Melenkevitz and Muthukumar differ from the more accurate results obtained from numerical solution of the mean-field equations of section II. Melenkevitz and Muthukumar find $d/R_g \propto (\chi N)^{\alpha}$, with $\alpha = 0$ for $10.5 < \chi N < 12.5$, $\alpha = 0.22$ for $12.5 < \chi N < 100$, and $\alpha = 0.17$ for $\chi N > 100$. These results differ significantly from the results shown in Figure 2, where α is seen to decrease monotonically from a value of 0.45 at the critical point. Thus, while Melenkevitz and Muthukumar are able to recover the correct mean-field scaling behavior in the strong segregation regime, the magnitude of L/R_g in this regime is underestimated in their treatment. At $\chi N = 125$, for example, they find $L/R_g = 5.10$, whereas numerical solution of the mean-field equations gives $L/R_g = 5.96$. Similar errors will be introduced whenever a truncated expansion of eq 27 is extended into the strong segregation regime as, for example, in the theory of Ohta and Kawasaki.[23] Failure of the Melenkevitz and Muthukumar theory to give the correct values for L/R_g very close to the critical point, where the order parameter is small and the fourth-order expansion is valid, cannot be traced to the truncation of the free energy expansion. Results obtained in this regime must instead be affected by the other approximations that are made in their treatment.

Treatments based on the free energy expansion of eq 27 are still quite useful, provided that one is interested in regimes where the order parameter is small and that one is careful in making additional approximations. The primary advantage of this technique over complete solution of the mean-field equations is the straightforward manner by which expressions can be obtained for the free energy of three-dimensional morphologies, i.e., those characterized by a set of Fourier components which are not collinear. In principle, the assumption of planar symmetry utilized in the derivation of the mean-field equations in section II can be removed by allowing the distribution functions, volume fractions, and mean fields to be functions not only of a single x coordinate but of the y and z coordinates as well. Considerable mathematical complexity is introduced in this manner, however, and the computing time required to obtain the numerical solution to these equations is increased enormously. Thus, in the present paper we have considered only the one-dimensional, lamellar morphology, whereas Leibler was able to consider cylindrical and spherical morphologies as well. For the symmetric case studied in detail here, the lamellar phase is always found to be the most stable phase. This situation changes for asymmetric copolymers, however, where three-dimensional morphologies were found to be more stable than the one-dimensional, lamellar morphology. Study of these types of systems in the weak segregation regime might be more easily accomplished by a progressively more detailed study of the free energy expansion of eq 27.[24]

Fluctuation Effects. Mean-field theory neglects fluctuation effects which have recently been shown to be important for bulk copolymer melts near the order–disorder transition.[25,26] Fluctuations stabilize the disordered phase so that a first-order transition to the ordered phase occurs at values of χN which are higher than those predicted by mean-field theory. Mean-field theory can clearly not be used to predict the value of χN for which a fluctuation-induced transition from the ordered phase to the disordered phase will take place. Some useful information may still be obtained, however, in the region where mean-field theory predicts an ordered phase but the copolymer actually exists in a disordered phase due to fluctuation effects. Specifically, one expects that the preferred wavelength of these fluctuations might be closely related to the repeat period calculated for the ordered phase in mean-field theory. The primary difference between fluctuations in a disordered phase and a repeat period in a ordered phase involves the coherence of composition oscillations; ordered phases consist of composition oscillations which are coherent over large length scales, whereas fluctuations in a disordered phase represent incoherent composition oscillations which average to zero. Similarity between these two types of composition oscillations is consistent with experiments which indicate that there is no noticeable discontinuity in q^* at the order–disorder transition.[26,27] Here q^* is the scattering vector for which the scattered intensity is a maximum and is inversely related to the preferred wavelength of the relevant composition oscillation. Experimentally q^* scales as $N^{-0.5}$ for low N, a result which is consistent with the fact that q^* is a function only of R_g in a completely homogeneous phase. Within a certain range on either side of the order–disorder transition, q^* is found to vary as $N^{-0.8}$. This scaling is roughly consistent with the mean-field scaling of q^* (with $q^* \propto 1/L$) for symmetric diblock copolymers in the weak segregation regime. One possible interpretation of this result is that the crossover from $N^{-0.5}$ scaling to $N^{-0.8}$ occurs at the value of N where fluctuation effects become important. Mean-field theory may qualitatively predict the molecular weight dependence of the wavelength of the preferred composition oscillation, even though the actual value of N at the transition between the ordered and disordered phases cannot be predicted.

Strong surface fields responsible for the ordering of block copolymers near surfaces are expected to suppress the relative importance of fluctuations in the surface region. For this reason, many of the results discussed in sections IV and V are not expected to be significantly affected by fluctuation corrections. Evidence for the suppression of fluctuation effects in thin films exists in the recent work of Russell et al., where neutron reflectivity was used to study ordering of thin films of symmetric polystyrene/poly(methyl methacrylate) (PS/PMMA) diblock copolymers.[28] Ordering originates from each of the film surfaces, with PMMA existing preferentially at the substrate surface and PS existing preferentially at the air surface. The degree of order increases with decreasing temperature (increasing χN), with details of the ordering depending on the proximity to a thickness-dependent transition temperature. The transition temperature decreases with increasing film thickness until it reaches its bulk value for very thick films. This behavior can be explained in terms of the decreasing importance of fluctuations as the film thickness decreases. As mentioned above, these fluctuations stabilize the disordered phase and are responsible for the first-order character of the order–disorder transition in symmetric diblock copolymers. As the film becomes thinner these random concentration fluctuations are overwhelmed by the order imposed by the film surfaces. As a result, the disordered phase becomes less stable and the transition temperature increases.

Thickness Instabilities in Thin Films. Complete orientational order in thin films of strongly segregated diblock copolymers is now well documented. As illustrated by Figure 8, the free energy of such a thin film is minimized by certain discrete film thicknesses which are related to the bulk repeat period of the diblock copolymer. Russell and co-workers have shown that for the PS/PMMA system

the ordering can be made to propagate throughout the entire film.[8,29] Thin films which have original thicknesses not equal to one of the quantized free energy minima will, after thermal equilibration, consist of regions of two discrete thicknesses corresponding to neighboring free energy minima. Typical films contain "islands" of increased film thickness or "holes" of decreased film thickness, depending on the average thickness of the film. These islands or holes grow over time and can be used to study coarsening in an idealized two-dimensional system.[30,31] Nucleation of islands or holes in films which contain several repeat periods generally occurs as the ordered lamellae orient themselves parallel to the surface. Nucleation is therefore a complicated process which is very difficult to control.

An interesting alternative to the study of films which initially contain islands or holes is to study films that roughen due to a thickness instability. Such a thickness instability will exist whenever the free energy as a function of thickness has a negative curvature. Consider, for example, a symmetric film with $\chi N = 9$ for which the B component is attracted to each surface. The negative curvature of γ as a function of d near the free energy maximum at $d = 4.95R_g$ (Figure 8a) indicates that films of this thickness will be unstable with respect to small thickness oscillations. One can therefore construct a stability analysis similar to that used to describe the spinodal decomposition of a binary blend,[32] where the composition of the blend is replaced by the thickness of the thin film. Consider a sinusoidal thickness variation in a film of average thickness d_o:

$$d(x) = d_0 + K \sin(kx) \tag{31}$$

The expression for ΔF_{osc}, the increase in free energy due to the thickness oscillation, contains a local term and a squared gradient term:

$$\Delta F_{osc} = \frac{A}{\lambda}\int_0^{\lambda}\left\{\gamma(d) - \gamma(d_0) + \kappa\left\{\frac{\partial d}{\partial x}\right\}^2\right\} dx \tag{32}$$

Here $\gamma(d)$ is the interfacial free energy as calculated in section V, λ is the wavelength of the oscillation ($\lambda - 2\pi/k$), and A is the total projected area of the oscillation. Expansion of $\gamma(d)$ about d_0 gives

$$\gamma(d) - \gamma(d_0) = \frac{1}{2}\frac{\partial^2\gamma}{\partial d^2}(d - d_0)^2 \tag{33}$$

The coefficient κ in the squared gradient term is determined by the increase in free energy associated with the formation of an increased surface area. This increased surface energy is given by $\gamma_0\{1 + (\partial d/\partial x)^2 - 1\}^{1/2}$, where γ_0 is the surface free energy for the polymeric component existing at the free surface. For small $\partial d/\partial x$ this increased surface energy is equal to $(\gamma_0/2)(\partial d/\partial x)^2$. The coefficient of the squared gradient term is therefore $\gamma_0/2$, and the complete expression for the free energy associated with the thickness oscillation is

$$\Delta F_{osc} = \frac{AK^2}{2\lambda}\int_0^{\lambda}\sin^2(kx)\left\{\frac{\partial^2\gamma}{\partial d^2} + \gamma_0 k^2\right\} dx \tag{34}$$

Thickness oscillations are unstable if the bracketed quantity in eq 34 is negative. One therefore obtains the following simple relationship for k_{crit}, the critical value of k below which composition oscillations are unstable:

$$k_{crit} = \left\{\frac{-1}{\gamma_0}\frac{\partial^2\gamma}{\partial d^2}\right\}^{1/2} \tag{35}$$

Detailed analysis of the free energy curves in Figure 8 at the first free energy maximum gives $\partial^2\gamma/\partial d^2 \simeq -0.5k_BT/VR_g$ for $\chi N = 9$, $\partial^2\gamma/\partial d^2 \simeq -1.5k_BT/VR_g$ for $\chi N = 10.5$, and $\partial^2\gamma/\partial d^2 \simeq -7k_BT/VR_g$ for $\chi N = 12$. The wavelength of the critical instability ($\lambda_{crit} = 2\pi/k_{crit}$) for a copolymer with a molecular weight of 30 000 varies from $\simeq$0.3 μm at χN = 9 to 0.1 μm at $\chi N = 12$, with $\gamma_0 = 30$ dyn/cm, $V = 4.8 \times 10^4$ Å^3, $R_g = 46$ Å, and $T = 150$ °C. These parameters are roughly consistent with a 30 000 molecular weight PS/PMMA block copolymer, for which $\chi N \simeq 10.5$.[33] The critical wavelengths for systems which can be studied experimentally are therefore expected to be of the order of tenths of micrometers.

Thickness oscillations with wavelengths larger than the critical values are predicted to be unstable, provided that the original film thickness corresponds to the first maximum in the free energy curve and that one of the components of the block copolymer is strongly attracted to each surface of the thin film. The equilibrium analysis derived here is appropriate only when the copolymer can achieve its equilibrium ordering throughout the thickness of the film over time scales which are short compared to the growth of a thickness oscillation. This condition is not expected to be met for maxima corresponding to transitions between films with multiple repeat periods. Transitions between these states are first order in character and require large-scale rearrangements of the copolymer chains. For these films the appearance of discrete thickness nonuniformities is expected to be coupled to the ordering of the film itself, with nucleation of islands or islands taking place during the actual ordering process. Growth of film thickness oscillations via a spinodal decomposition mechanism should be observable for films containing a single oscillation, where the decomposition is as illustrated in Figure 10. The driving force for the decomposition process is contained in the curve of $\Delta\gamma$ vs film thickness, which can be derived in general for all values of N_a, N_b, and χ, and for asymmetric systems for which the quantity $a^2\rho_0$ is different for each polymer (see Appendix 2). Results can also be obtained for all values of the surface interactions, including those which favor enrichment of different components at the two separate interfaces. The rate of the decomposition process will be governed by this driving force and by a two-dimensional diffusion process that governs the transport of copolymer chains between regions of different film thickness. Study of the growth of these thickness instabilities by X-ray or neutron reflectivity[34] or by atomic force microscopy[35] may therefore be a very useful method by which the dynamics of very thin films can be probed.

VII. Summary

Mean-field theory gives valuable insights into the bulk, surface, and thin film properties of block copolymer melts. Results free from additional approximation have been obtained by using numerical techniques to solve a set of equations involving the polymer chain probability distribution functions. Solutions can be obtained for diblock copolymers of varying asymmetry but have been given only for symmetric diblock copolymers to illustrate some fundamental aspects of the mean-field behavior of block copolymer melts. The most important results of this work are as follows.

Bulk Melts. We obtain the true mean-field predictions for the weak segregation regime. Composition oscillations are found to vanish continuously at the critical point predicted by Leibler ($\chi N = 10.495$). The equilibrium repeat period scales as $R_g(\chi N)^{\alpha}$, where α varies continuously from 0.45 at the critical point to 0.17 in the strong

segregation regime, where the results of Helfand and Wasserman are recovered. Detailed composition profiles are obtained for all values of χN. For $\chi N > 20$ a repeat period consists of pure A and B microdomains separated by an interfacial region characterized by a hyperbolic tangent profile. The width of this region approaches the width between infinite molecular weight A and B homopolymers as χN approaches infinity but is still 10% greater than this limiting value for $\chi N = 160$.

Surfaces. Surfaces that have a preferential affinity for one of the components of the block copolymer will induce composition oscillations in the near surface region. The manner in which these oscillations decay into the bulk is determined by the proximity to the bulk order–disorder transition. Details of the surface profile are in quantitative agreement with those of an earlier theory of Fredrickson, provided that the maximum order parameter is less than 0.1. Discrepancies in the results obtained from the two treatments are indicative of the failure of weak segregation theories to account for systems with a high degree of order. Numerical solution of the mean-field equations gives predictions which are quantitative, regardless of the degree of order.

Thin Films. The behavior of thin block copolymer films is governed by the close proximity of the two film surfaces. Interference between composition oscillations originating from the two surfaces gives rise to thickness oscillations in the total interfacial free energy of the film. Thin block copolymer films will in general separate into regions of different thicknesses to minimize this total interfacial free energy. For thin films with multiple repeat periods, nucleation of discrete thickness regions is expected to take place as the equilibrium thin film ordering is established. An instability mechanism by which thickness variations may be induced in weakly ordered thin films consisting of a single repeat period is postulated. Small-amplitude thickness oscillations with wavelengths greater than some critical value are predicted to be unstable, provided that the original film thickness corresponds to the first free energy maximum in the interfacial free energy as a function of film thickness.

Acknowledgment. I have benefited from helpful discussions with A. M. Mayes and T. P. Russell.

Appendix 1: Extension to Multicomponent Systems

Extension of the self-consistent mean-field equations to multicomponent systems is straightforward, provided that the equations are cast in an appropriate form. Generalization of the equations in this way allows one to examine the properties of an enormous number of systems, including random copolymers, multiblock copolymers, and copolymer/homopolymer blends. The form described here is similar to that utilized in a recent theory of block copolymers at the interface between immiscible homopolymers.[3] Each distinct polymeric component k will be described by two distribution functions, q_{k1} and q_{k2}. The governing equation for any distribution function is as described in the body of the paper. For q_{k1} one has

$$q_{k1}(i,j) = \left\{\frac{1}{6}q_{k1}(i-1,j-1) + \frac{1}{6}q_{k1}(i+1,j-1) + \frac{4}{6}q_{k1}(i,j-1)\right\}\exp\{-w(i,j)/k_BT\} \quad \text{(A1)}$$

with a similar equation for q_{k2}. Thermodynamic interactions with all different segment types must now be accounted for in the equation for the mean field. The j dependence of the mean field is determined entirely by the type of repeat unit represented by j. This fact is taken into account through the expanded notation $w(i, p(j))$, where p designates the type of repeat unit being considered. For A/B diblock copolymers p must be either A or B. Mean fields are related to chemical potentials, which for a homogeneous system can be written in the following generalized form:[36]

$$\frac{\mu_k}{k_BT} = \ln \phi_k + 1 - N_kK_\phi + \frac{1}{k_BT}\sum_{j=1}^{N_k} w^\circ(p(j)) \quad \text{(A2)}$$

The first three terms in eq A2 are associated with the entropic contributions to the free energy, with K_ϕ defined as follows:

$$K_\phi = \sum_k \frac{\phi_k}{N_k} \quad \text{(A3)}$$

The last term in eq A2 is the enthalpic part of the chemical potential, given as follows:

$$\frac{w^0(p)}{k_BT} = \frac{1}{2}\sum_{m\neq n}\{\phi_m - \delta(m-p)\}\chi_{mn}\{\phi_n - \delta(n-p)\} \quad \text{(A4)}$$

Here ϕ_m represents the overall volume fraction of the chemical species m, and the summation is over all possible species (A, B, C, etc.). The delta functions are defined so that $\delta(m-p) = 1$ for $m = p$ and $\delta(m-p) = 0$ for $m \neq p$. The hypothetical reference state for which $\mu_k = 0$ is a pure polymer melt for which the interactions characterized by the χ parameters have been turned off. With this reference state, the free energy density of a homogeneous mixture of polymers is given by the familiar Flory–Huggins form:

$$\frac{f}{k_BT\rho_0} = \sum_k \phi_k \ln \phi_k + \frac{1}{2}\sum_{m\neq n}\chi_{mn}\phi_m\phi_n \quad \text{(A5)}$$

The mean fields include K_ϕ from the entropic contribution, the enthalpic contribution $w^\circ(p(j))$, and the contribution Δw associated with the incompressibility constraint. For an inhomogeneous system these components are all functions of the position i

$$w(i,j) = w^0(i,p(j)) - k_BTK_\phi(i) - \Delta w(i) \quad \text{(A6)}$$

with

$$\frac{\Delta w}{k_BT} = \zeta\left\{\sum_k \phi_k(i) - 1\right\} \quad \text{(A7)}$$

The volume fraction corresponding to the qth repeat unit along a polymer chain is given by

$$\phi_k(i,j) = (1/N_k)\exp(\mu_k/k_BT - 1)q_{k1}(i,j)q_{k2}(i,N-j) \quad \text{(A8)}$$

with the volume fraction of any given portion of a polymer chain being given by the summation over the relevant repeat units. The volume fraction of polymer k, for example, is given by the summation of all N_k repeat units:

$$\phi_k(i) = \sum_{j=1}^{N_k}\phi_k(i,j) = \frac{1}{N_k}\exp(\mu_k/k_BT - 1)\sum_{j=1}^{N_k} q_{k1}(i,j)q_{k2}(i,N-j) \quad \text{(A9)}$$

As discussed elsewhere the mean fields are specified only to within an additive constant.[3,14] Addition of a constant factor A_k to the mean field as given by eq A6 can be compensated for by adding a constant factor of N_kA_k

to the factor appearing in the exponential of eq A8. The generalized equations given here differ slightly from the equations given in the text in that a constant factor of $1/N_k$ has been subtracted from the mean fields to obtain a form which depends only on the type of repeat unit being considered and not on the degree of polymerization of the polymer chain of which it is a part. The two treatments are mathematically identical and give exactly the same results.

Appendix 2: Extension to Polymers with Dissimilar Dimensions

The derivation presented thus far is valid when polymer repeat units of all types are characterized by the same value of the quantity $\rho_0 \mathbf{a}^2$. This assumption simplifies the mathematics but must not necessarily be made. In fact, this sort of asymmetry in the chain flexibility was included by Helfand and Wasserman in the expression for the free energy of a lamellar copolymer phase in the narrow interphase approximation, from which the solid line in Figure 2 was derived.[6] In addition, Helfand and Sapse have derived analytic expressions for the infinite molecular weight limit of the interfacial free energy between homopolymers characterized by different values of $\rho_0 \mathbf{a}^2$.[2,37] Helfand and co-workers expressed the chain flexibility in terms of a parameter β, defined as follows:

$$\beta^2 = \frac{1}{6}\rho_0 \mathbf{a}^2 \tag{A10}$$

For $\beta_a = \beta_b$, there is no ambiguity in the definition of the statistical length of a repeat unit, since this length is determined by specification of ρ_0. For $\beta_a \neq \beta_b$, the parameters are again specified in terms of ρ_0 but in a more complicated manner. The degrees of polymerization of the copolymer blocks are defined so that the respective volumes of the A and B blocks are N_a/ρ_0 and N_b/ρ_0. We then reference the lattice to the A repeat units, with the distance between lattice layers being equal to the statistical segment length of an A repeat unit:

$$\Delta x = \beta_a(6/\rho_0)^{1/2} \tag{A11}$$

For both types of repeat units to be placed on the same lattice, the degree of polymerization of the B block must be rescaled to N_b' so that the statistical length of a B repeat unit is also equal to Δx

$$\Delta x = \beta_b(6/\rho_0')^{1/2} \tag{A12}$$

with $\rho_0' = \rho_0(N_b'/N_b)$. The rescaled degree of polymerization N_b' is determined by combination of eqs A11 and A12. For the general case of a repeat unit of type k, one obtains

$$N_k' = N_k(\beta_k^2/\beta_a^2) \tag{A13}$$

The generalized self-consistent mean-field equations of Appendix 1 must be modified in two minor ways to take into account the asymmetry in the polymer chain flexibility. First, the equation for the mean fields must be multiplied by N_k/N_k' to account for the corresponding increase in size of the repeat unit:

$$w(i,j) = \frac{N_k}{N_k'}\{w^0(i,p(j)) - k_B T K_\phi(i) - \Delta w(i)\} \tag{A14}$$

In addition, the summation over N_k repeat units in the expression for ϕ_k must be replaced by a summation over the N_k' rescaled repeat units as

$$\phi_k(i) = \sum_{j=1}^{N_k'} \phi_k(i,j) \tag{A15}$$

with

$$\phi_k(i,j) = (\beta_a^2/N_k\beta_k^2)\exp(\mu_k/k_B T - 1)q_{k1}(i,j)q_{k2}(i,N_k'-j) \tag{A16}$$

As usual, the χ parameter is defined in terms of the interaction between segments with a volume of $1/\rho_0$, with the free energy of a homogeneous system given by eq A5.

References and Notes

(1) Russel, W. B.; Saville, D. A.; Schowalter, W. R. *Colloidal Dispersions*; Cambridge University Press: Cambridge, 1989.
(2) Brown, H. R. *Macromolecules* **1989**, *22*, 2859.
(3) Shull, K. R.; Kramer, E. J. *Macromolecules* **1990**, *23*, 4769.
(4) Leibler, L. *Macromolecules* **1980**, *13*, 1602.
(5) Helfand, E. *Macromolecules* **1975**, *8*, 552.
(6) Helfand, E.; Wasserman, Z. R. *Macromolecules* **1976**, *9*, 879.
(7) Fredrickson, G. H. *Macromolecules* **1987**, *20*, 2535.
(8) Coulon, G.; Russell, T. P.; Deline, V. R.; Green, P. F. *Macromolecules* **1989**, *22*, 2581.
(9) Helfand, E.; Tagami, Y. *Polym. Lett.* **1971**, *9*, 741.
(10) Helfand, E.; Tagami, Y. *J. Chem. Phys.* **1972**, *56*, 3592.
(11) Helfand, E. *J. Chem. Phys.* **1975**, *62*, 999.
(12) Scheutjens, J. M. H. M.; Fleer, G. J. *J. Phys. Chem.* **1979**, *83*, 1619.
(13) Scheutjens, J. M. H. M.; Fleer, G. J. *J. Phys. Chem.* **1980**, *84*, 178.
(14) Hong, K. M.; Noolandi, J. *Macromolecules* **1981**, *14*, 727.
(15) Shull, K. R. *J. Chem. Phys.* **1991**, *94*, 5723.
(16) Edwards, S. F. *Proc. Phys. Soc. London* **1965**, *85*, 613.
(17) Semenov, A. N. *Sov. Phys. JETP* **1985**, *61*, 733.
(18) Schmidt, I.; Binder, K. *J. Phys. (Paris)* **1985**, *46*, 1631.
(19) Fredrickson, G. H.; Helfand, E. *J. Chem. Phys.* **1987**, *87*, 697.
(20) Mayes, A. M.; Olvera de la Cruz, M. *Macromolecules* **1991**, *24*, 3975.
(21) Mayes, A. M. Personal communication.
(22) Melenkevitz, J.; Muthukumar, M. *Macromolecules* **1991**, *24*, 4199.
(23) Ohta, T.; Kawasaki, K. *Macromolecules* **1986**, *19*, 2621.
(24) Olvera de la Cruz, M. *Phys. Rev. Lett.* **1991**, *67*, 85.
(25) Bates, F. S.; Rosedale, J. H.; Fredrickson, G. H.; Glinka, C. J. *Phys. Rev. Lett.* **1988**, *61*, 2229.
(26) Bates. F. S.; Rosedale, J. H.; Fredrickson, G. H. *J. Chem. Phys.* **1990**, *92*, 6255.
(27) Almdal, K.; Rosedale, J. H.; Bates, F. S.; Wignall, G. D.; Fredrickson, G. H. *Phys. Rev. Lett.* **1990**, *65*, 1112.
(28) Menelle, A.; Russell, T. P.; Anastasiadis, S. H.; Satija, S. K.; Majkrzak, C. F. *Phys. Rev. Lett.* **1992**, *68*, 67.
(29) Russell, T. P.; Coulon, G.; Deline, V. R.; Miller, D. C. *Macromolecules* **1989**, *22*, 4600.
(30) Ausserre, D.; Chatenay, D.; Coulon, G.; Collin, B. *J. Phys. (Paris)* **1990**, *51*, 2571.
(31) Coulon, G.; Collin, B.; Ausserre, D.; Chatenay, D.; Russell, T. P. *J. Phys. (Paris)* **1990**, *51*, 2801.
(32) Porter, D. A.; Easterling, K. E. *Phase Transformations in Metals and Alloys*; Van Nostrand Reinhold: New York, 1981.
(33) Russell, T. P.; Hjelm, R. P.; Seeger, P. A. *Macromolecules* **1990**, *23*, 890.
(34) Russell, T. P. *Mater. Sci. Rep.* **1990**, *5*, 171.
(35) Maaloum, M.; Ausserre, D.; Chatenay, D.; Coulon, G. Preprint.
(36) Evers, O. A.; Scheutjens, J. M. H. M.; Fleer, G. J. *Macromolecules* **1990**, *23*, 5221.
(37) Helfand, E.; Sapse, A. M. *J. Chem. Phys.* **1975**, *62*, 999.